Aeroelastic System Control by a Multiple Spoiler Actuation and MRAC Scheme

Aeroelastic System Control by a Multiple Spoiler Actuation and MRAC Scheme

M. Cassaro[1] and M.Battipede[2]
Politecnico di Torino, Turin,10128, Italy

P. Marzocca[3]
Aerospace and Aviation Program, RMIT University, Bundoora VIC 3083, Australia

and

G. Ahmadi[4]
Clarkson University, Potsdam, NY, 13699, USA

A novel wing configuration to control flutter and post-flutter limit cycle oscillations is proposed. The new wing consists of a multiple spoiler control surface, with a predefined and coordinated actuation strategy. The proposed architecture, optimized through CFD analysis, is fabricated and tested in the wind tunnel to validate the aerodynamic properties of the wing section. The experimentally obtained nonlinear aerodynamic database is implemented in a simulation environment, which is used to investigate the dynamic response of the proposed wing configuration aeroelastic model. The coupled, two degree of freedom, structural model has nonlinear plunging/pitching characteristics, which allow the system to exhibit LCOs above flutter speed. The open and closed loop responses of the system are investigated and compared to a trailing-edge flap solution of the same wing section. The regulation problem is obtained for a normalized MRAC scheme, modified for performance improvement. The same algorithm is applied to both plants and results validate the robustness and the adaptation capabilities of the implemented control scheme. Further sensitivity analyses to external disturbances, which are different gust distributions, demonstrate the efficacy and solidity of the overall configuration investigated.

Nomenclature

A.C.	=	wing aerodynamic center
a	=	dimensionless distance between the mid-chord and the elastic axis
b	=	semi-chord of airfoil
$c.g.$	=	wing center of gravity
C_h C_θ	=	structural damping coefficients in plunging and pitching
C_L C_m	=	lift and moment coefficients
C_{L_β} C_{m_β}	=	lift and moment curve slopes per trailing-edge flap deflection
CFD	=	Computational Fluid Dynamics
h	=	plunging displacement
α	=	angle of attack (AoA)
α_e	=	effective angle of attack

[1] Ph.D Candidate, Department of Mechanical and Aerospace Engineering, C.so Duca degli Abruzzi 24. Visiting Scholar in the Mechanical and Aeronautical Engineering Department at Clarkson University.
[2] Associate Professor, Department of Mechanical and Aerospace Engineering, C.so Duca degli Abruzzi 24. Associate Fellow AIAA.
[3] Professor and Deputy Head of School (Aerospace and Aviation), School of Aerospace, Mechanical and Manufacturing Engineering PO BOX 71 Bundoora VIC 30833 Australia. Associate Fellow AIAA.
[4] Professor, Department of Mechanical and Aeronautical Engineering, 8 Clarkson Avenue.

β = flap angle
θ = pitch angle
I_α = mass moment of inertia of airfoil about elastic axis
k_h k_θ = structural spring stiffnesses in plunging and pitching
L = lift
M = aerodynamic moment, computed with respect to the elastic axis
m_t = total mass of the system
m_w = mass of the airfoil
PID = proportional-integral-derivative
Re = Reynolds number
U = free stream velocity
$w_g(\tau)$ = gust velocity distribution
x_θ = dimensionless distance from elastic axis to mid-chord, positive rearward
ρ = air density

I. Introduction

The aeroelastic instabilities and their control are topics that attracted considerable attention in the aerospace scientific literature in the last decade. In particular, aeroelastic phenomena such as divergence, flutter, and LCOs have been carefully investigated [1-3] and, for many cases, the instability boundaries were determined with reasonable accuracy, using theoretical and experimental techniques for various operation conditions. However, unpredictable structural damages can lead to unexpected aeroelastic behavior within the nominal flight envelope, which points to the importance of active control the response of the lifting surfaces to prevent any potential aeroelastic-derived failure. In these circumstances, changes in the structural properties modify the nonlinear system dynamic response, which requires robust adaptive control law to be handled properly. Different research teams have proposed different control laws and architectures, designed and tested both numerically, in simulation environment, and experimentally, with wind tunnel trials or flight-testing. In [4-6] the authors developed and tested their control algorithms for the Benchmark Active Control Technology (BACT) Wind-Tunnel Model, while in [7-9] the authors designed and tested their control laws for the Nonlinear Aeroelastic Testbed Apparatus (NATA) [10] at Texas A&M University. In [11] the authors tested and validated several adaptive control architectures on similar 2D aeroelastic model. The control systems developed, including the most recent neural network [12], adaptive back-stepping [13] and L_1 adaptive controller [14], have been applied to wing models, in simulation or experimental setup, with either a single trailing edge control surface or a combination of leading and trailing edge control surfaces. Some issues related to the latter solutions can be highlighted; these are trailing edge flap saturation, being the flap displacement usually constrained between +/- 10 degrees, and leading edge slat actuation system complexity. The work presented in this paper investigates the effectiveness of an original configuration, which would represent a possible alternative and a solution to the previous mentioned issues. Specifically, a novel coordinated multiple spoiler actuation strategy for flutter suppression, is evaluated. A cross simulation/experimental approach is used to obtain the final configuration of the actuation system. The innovative test article consists of a wing section equipped with multiple-spoilers installed on a strip, located at the 15% of the chord length, with a predefined and coordinated actuation strategy. The proposed architecture, optimized through computational fluid dynamics (CFD) analysis, is fabricated and tested in the wind tunnel to validate the aerodynamic properties of the wing section. The experimentally obtained nonlinear aerodynamic database is used in conjunction with a classical nonlinear plunging/pitching structural model, implemented in a simulation environment, to investigate the dynamic response of the proposed wing configuration aeroelastic model. The resulting aeroelastic model exhibits a supercritical Hopf-bifurcation behavior, that is a stable Limit Cycle Oscillations (LCOs) past the flutter speed. The open and closed loop responses of the system are investigated and compared to a trailing-edge flap solution of the same wing section. The regulation problem is obtained for a normalized Model-Reference-Adaptive-Controller (MRAC) scheme, modified for performance improvement [11]. The same algorithm is applied to both plants to validate the robustness and the adaptation capabilities of the implemented control scheme. Sensitivity analyses to external gust disturbances, demonstrate the efficacy and solidity of the overall configuration investigated.

II. Aeroelastic Model

The aeroelastic system under examination consists of a two degree of freedom (DOF), nonlinear plunging/pitching structural model coupled to the aerodynamic model representative of the real, wind tunnel tested, prototype of the proposed wing configuration. The design process, as reported in [15], went through several steps aiming to optimize

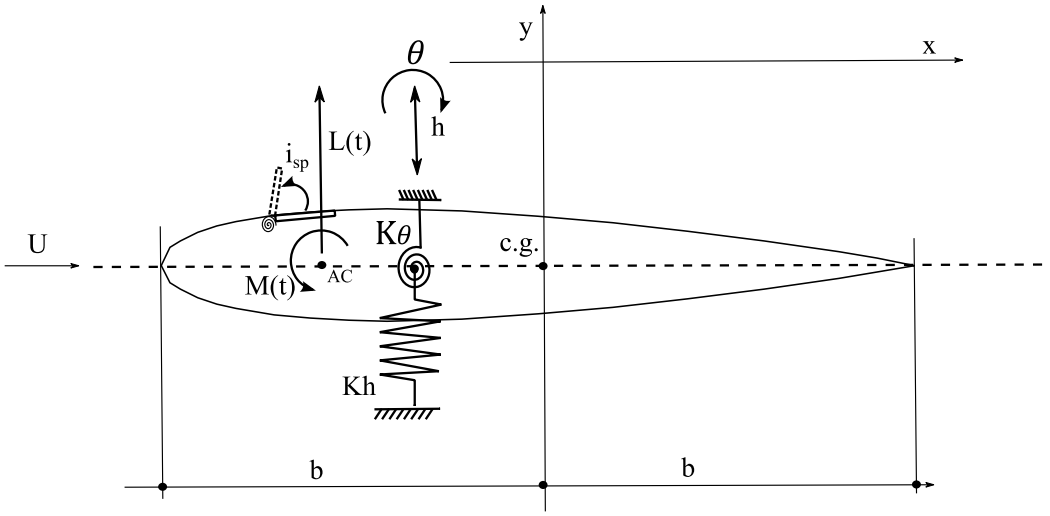

Figure 1. 2D aeroelastic wing-spoiler configuration schematic.

the flutter control capabilities for a finite rectangular wing with a NACA0024 airfoil using multiple coordinated spoilers. The particular choice of airfoil was due to the actuators (linear solenoid push-type actuators) and the space requirements for their installation. The spoiler location, 15% of the chord length from the leading edge, as well as their size and the opening angle, are the results of CFD analyses carried out with the objective of maximizing the produced pitching moment while minimizing the drag. The prototype has five different spoiler sections, installed in series covering the entire wingspan length. This solution allows the individual actuation of spoilers to provide a range of lift and moment increments, ΔC_L and ΔC_m in terms of coefficients, differently from the operation of a single, gradually activated spoiler. The spoiler stripe has also a predesigned opening strategy intended to preserve pressure distribution symmetry on the wing upper surface, so to avoid undesirable roll moment[15]. Numbering the spoilers progressively, 1 to 5, from left to right along the wing section span, the opening strategy sequence is: spoiler #3, #2-4, #1-3-5,#1-2-4-5 and finally #1-2-3-4-5. The schematic view of the aeroelastic configuration described is reported in Figure 1, where the i_{sp} parameter is the number of active spoiler. The plunging $h\ (m)$, positive downward, and pitching $\theta\ (rad)$, measured from the horizontal at the elastic axis of the airfoil and positive nose up, displacements are restrained by a pair of springs attached to the elastic axis (EA) of the airfoil with spring constants, $k_h\ (N \cdot m^{-1})$ and $k_\theta(\theta)\ (N \cdot rad^{-1})$, respectively. Here, $k_\theta(\theta)$ denotes a continuous, linear parameterizable nonlinearity, that is, the aeroelastic system has a continuous nonlinear (5th-order) restoring moment in the pitch degree of freedom (DOF). As explained afterward, the deduction and incremental values of lift and pitching moment, are functionally related to the i_{sp} parameter and the spoiler effectiveness factor $\left(k_{\delta_{sp}}\right)_L$, which takes into account of the selected spoiler opening sequence. Additionally, it should be noted that the actuator working frequencies are one order of magnitude faster than the aeroelastic properties of the model analyzed and for this reason will be neglected in the model dynamic equations. An existing wing section experimental test article is used, hence it was chosen not to describe the aerodynamic force and moment by any preexisting analytical unsteady or quasi-steady form [16-21] but rather, using an approach common in flight simulation [22], by the use of an aerodynamic database experimentally obtained by wind tunnel testing.

This approach allows us to include in the model nonlinearities given by stall and the actual contribution of the spoiler activation strategy to the aerodynamic loads. The equations describing the aeroelastic model in Fig. 1 are:

$$\begin{bmatrix} m_t & m_w x_\theta b \\ m_w x_\theta b & I_\theta \end{bmatrix} \begin{bmatrix} \ddot{h} \\ \ddot{\theta} \end{bmatrix} + \begin{bmatrix} c_h & 0 \\ 0 & c_\theta \end{bmatrix} \begin{bmatrix} \dot{h} \\ \dot{\theta} \end{bmatrix} + \begin{bmatrix} k_h(h) & 0 \\ 0 & k_\theta(\theta) \end{bmatrix} \begin{bmatrix} h \\ \theta \end{bmatrix} = \begin{bmatrix} -L \\ M \end{bmatrix} \qquad (1)$$

where $m_t\ (kg)$ is the total mass of the system, $m_w(kg)$ the mass of the airfoil, x_θ the dimensionless distance measured from the elastic axis to the center of mass, $I_\theta\ (Kg \cdot m^2)$ the mass moment of inertia of airfoil about elastic axis, $c_h\ (N \cdot m^{-1} \cdot s^{-1}), c_\theta(N \cdot s^{-1})$ the structural damping coefficients in plunging and pitching and the external aerodynamic force, $L\ (N)$, and moment, $M\ (N \cdot m)$, are expressed as a function of the lift and pitching aerodynamic moment coefficient and are written by the classical formulation per unit of length:

$$L = \rho U^2 b C_L\left(\alpha_e, Re, i_{sp}, w_G(\tau)\right),\ M = \rho U^2 b^2 C_m\left(\alpha_e, Re, i_{sp}, w_G(\tau)\right) \tag{2}$$

where $\alpha_e\ (rad)$ is the effective aerodynamic angle of attack, Re the Reynolds number and $w_G(\tau)$ the gust velocity profile.

The experimental aerodynamic coefficient dataset, obtained by means of a six axes wind tunnel force balance, are reported in Fig. 2. The measured aerodynamic angle of attack (AoA) domain is $\pm 18\ deg$. In the figure, the lines represent configurations going from 0 (clean) up to all 5 spoiler active. As can be noticed, with this approach, nonlinear stall region of the wing and the nonlinear effect of the spoiler activation are implicitly included in the formulation. The wing section in post-flutter conditions exhibits LCOs, hence it is assumed that the aerodynamic angle of attack α, used to interpolate the data can be written as:

$$\alpha = \left[\theta + \frac{\dot{h}}{U} + \left(\frac{1}{2} - a\right) b\left(\frac{\dot{\theta}}{U}\right)\right] \tag{3}$$

where θ is the geometrical pitch angle, a and $b\ (m)$ are respectively the dimensionless distance between the mid-chord and the elastic axis and the semi-chord of airfoil, and the contributions of both the plunge and pitching velocities are taken into account. The analytical expressions of the lift and aerodynamic moment factoring the experimentally evaluated coefficients are:

$$L = \rho U^2 b C_{L_\alpha}\left[\theta + \frac{\dot{h}}{U} + \left(\frac{1}{2} - a\right) b\left(\frac{\dot{\theta}}{U}\right)\right] - \rho U^2 b \Delta C_{L_{sp}} \tag{4}$$

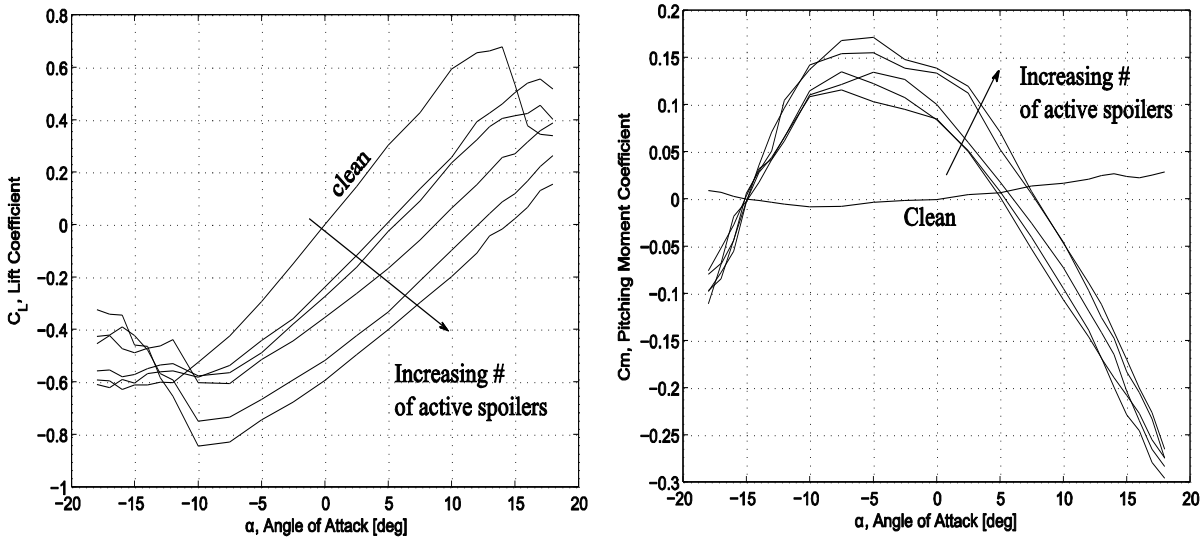

Figure 2. Aerodynamic database, lift and pitching moment coefficient experimental values.
Transition from clean to five open spoiler configuration is specified by the arrows.

$$M = \rho U^2 b^2 C_{m_\alpha} \left[\theta + \frac{\dot{h}}{U} + \left(\frac{1}{2} - a\right) b \left(\frac{\dot{\theta}}{U}\right)\right] + \rho U^2 b^2 \Delta C_{m_{sp}} \tag{5}$$

where $U\,(m/s)$ is the free stream velocity, c_{l_α} c_{m_α} are lift and moment coefficients of the airfoil and $\rho\ (Kg/m^3)$ is the air density. Herein, the contribution to lift and pitching aerodynamic moment of the spoiler is written as a function of the wing angle of attack, flight speed and number of spoiler opened. The general formulation describing the spoiler effect on lift coefficient is:

$$\Delta C_{L_{sp}} = \sum_{i\,=\,i_{sp}} \left(k_{\delta_{sp}}\right)_i \left(\Delta C_{L_{sp}}(\alpha)\right)_{\delta_{max}} \cdot \frac{(C_L)_M}{(C_L)_{M=0}} \left(\frac{L_E}{L_R}\right)_{sp} \tag{6}$$

where $\left(k_{\delta_{sp}}\right)_L$ is the single spoiler lift effectiveness factor, $\left(\Delta C_{L_{sp}}(\alpha)\right)_{\delta_{max}}$ is the single spoiler lift increment at maximum deflection for given AoA, $\frac{(C_L)_M}{(C_L)_{M=0}}$ takes into account of the compressibility, $\left(\frac{L_E}{L_R}\right)_{sp}$ of the flexibility of the wing section and the summation is extended to the number of operating spoiler panels, i_{sp}. In the wing configuration prototyped the spoiler works in a binary on/off mode, with maximum and unique deflection allowed at $85\ deg$, the airflow is uncompressible and the wing properties are lumped in a single 2D section, which is by definition rigid. Therefore, equation (6) reduces to

$$\Delta C_{L_{sp}} = \sum_{i\,=\,i_{sp}} \left(k_{\delta_{sp}}\right)_i \Delta C_{L_{sp}}(\alpha) \tag{7}$$

Analogous considerations are applied to the pitching moment coefficient, which final equation has exactly the same form

$$\Delta C_{m_{sp}} = \sum_{i\,=\,i_{sp}} \left(k_{\delta_{sp}}\right)_i \Delta C_{m_{sp}}(\alpha) \tag{8}$$

The nonlinear trend of the spoiler aerodynamic increments is attributed to the nonlinearity of the effectiveness factor, which varies with the number of the open spoilers, their location and consequently to the opening strategy [15]. To evaluate the robustness and effectiveness of the proposed architecture a wind gust model is introduced in the nonlinear equation system.

This means adding to the aerodynamic angle of attack, used to interpolate the coefficients database, the contribution given by the gust velocity profile, which in a two dimensional problem it is reduces to $\Delta\alpha_{gust} = \mathrm{atan}(w_G(\tau)/U)$. Herein $w_G(\tau)$ denotes the disturbance velocity (vertical direction only) and τ is a dimensionless time defined as $\tau = Ut/b$. Consequently, the effective angle of attack formulation α_e, adopted in the actual lift and aerodynamic moment expressions, is given as:

$$\alpha_e = \left[\theta + \frac{\dot{h}}{U} + \left(\frac{1}{2} - a\right) b \left(\frac{\dot{\theta}}{U}\right) + \Delta\alpha_{gust}\right]. \tag{9}$$

The proposed aeroelastic model, with the parameters set as in Table 1, exhibits periodic LCOs beyond a critical value of the free stream velocity U in the absence of wing gust, that is $U_{flutter} = 7.5\ m/s$. The uncontrolled plant response in both DOF is reported in Fig. 3 in the form of phase diagrams. In the comparative trailing-edge flap configuration, of the same aeroelastic system, the aerodynamic force and moment are modified to account for flap deflection effect. In particular, the terms $\Delta L_\beta = -\rho U^2 b C_{L_\beta}\beta$ and $\Delta M_\beta = \rho U^2 b^2 C_{m_\beta}\beta$, with $\beta\ (deg)$ the flap deflection angle and C_{L_β}, C_{m_β} the flap control derivatives, are added to the right hand side of Eq. (2), respectively

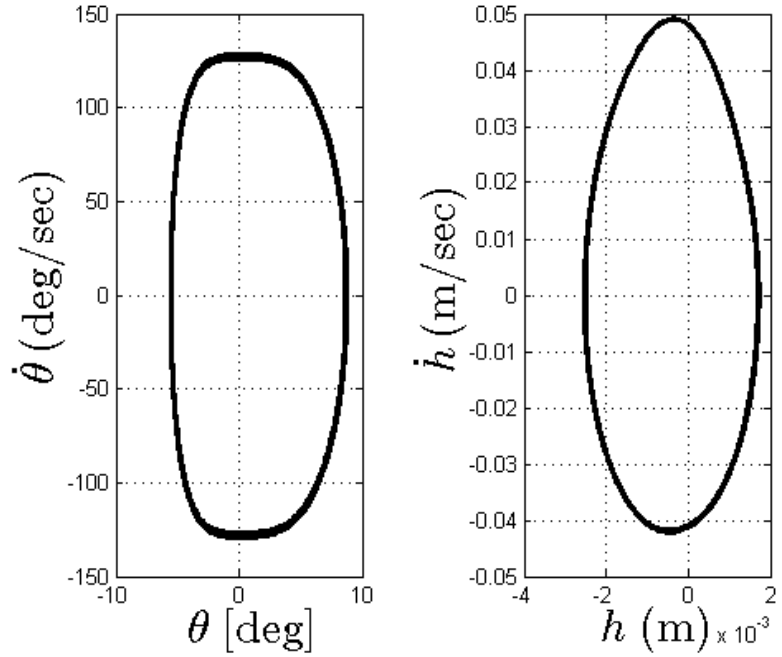

Figure 3. Aeroelastic Plant, uncontrolled LCOs response. *Pitch and plunge phase diagrams.*

to the lift and the aerodynamic moment equation [11]. Obviously, in this case, C_L and C_m are allowed to assume values belonging only to the clean configuration. The aeroelastic equation of motion (1) can be written into an equivalent state-space form, amenable for control law development purpose. That is,

$$\dot{x}(t) = Af(x,t)x(t) + Bg(x,t)u(t)\,; \quad y = [x_2\ x_4] \tag{10}$$

where $x(t) = [h\ \theta\ \dot{h}\ \dot{\theta}] \in \mathbb{R}^4$ is the state vector, $u(t) \in \mathbb{R}^1$ is the control input, $A \in \mathbb{R}^{4\times4}$ is the state matrix, B $\in \mathbb{R}^{4\times1}$ is control matrix, $f(x,t)$ and $g(x,t)$ are unknown functions collecting the nonlinearities and y is the designated output, in this case only $[\theta\ \dot{\theta}]$ are supposed to be available for closed-loop feedaback.

III. Modified Model Reference Adaptive Controller Application

To regulate the self-sustaining LCOs a control law must be associated to the spoiler's actuation system. Instead of the simple proportional integral derivative (PID) controller used in the first experimental evaluation of the novel architecture [15], which required a long tuning process for the complexity of the problem, an adaptive control architecture has been chosen for this application. In particular, an MRAC scheme, modified for performance improvement both in adaptation rate and tracking error, is selected. This choice is made for consistency of result comparison and validation purpose of the control law, since the same control architecture can be applied, with few modifications, to a trailing-edge flap configuration of the same wing. The latter represents the reference benchmark for results evaluation. The control objective, as literature suggests [4-14], is to regulate to zero the pitch angle θ, while adaptively compensating for uncertainties and nonlinearities in the model parameters. It has been already proven, that controlling θ is sufficient to regulate simultaneously also the plunge displacement h. As a result, only the pitch angle and its derivative, are consider observable, so that $x_{obs} = [\theta\ \dot{\theta}]$. The MRAC scheme control problem formulation, as reported in [23] consist in designing $u(t)$ such that all the states $x(t)$ in the closed-loop system are uniformly bounded and track the state vector of a desired reference model

$$\dot{x}_m(t) = A_m x_m(t) + B_m r(t), \qquad x_m(0) = x_0 \tag{11}$$

The standard solution for this problem is:

$$u(t) = -\hat{\theta}^T(t)x(t) + k_0 r(t) \tag{12}$$

where $\hat{\theta}(t)$ is the estimate of the unknown parameters $\theta^*(t)$, which is the adaptation parameter vector. However, as far as a regulation problem is concerned, when the term $k_0 r(t)$ goes to zero the solution reduces to $u(t) = -\hat{\theta}^{\mathrm{T}}(t)x(t)$. Performance improvement is obtained by enriching the control signal with an extra term as hereafter described. Equation (10) belongs to a class of plant that can be rewritten in an amenable form to model reference control schemes as

$$\dot{x}(t) = A_m x(t) + B\theta^{*\mathrm{T}} x(t) + Bu(t) \tag{13}$$

where $x \in \mathbb{R}^n$ is the state vector, assumed to be measurable, $u \in \mathbb{R}$ is the control input, $\theta^* \in \mathbb{R}^n$ is an unknown parameters vector belonging to a known compact convex set $\Omega \subset \mathbb{R}^n$, $A_m \in \mathbb{R}^{n\times n}$ is Hurwitz and $B \in \mathbb{R}^n$ are known and the pair $(A_m;\ B)$ is controllable. As proved in [23], the fact that the parameter θ^* appears linearly in Eq. (13) does not mean that the dynamics are linear. It is straightforward to show that Eq. (11) can be rearranged to obtain the parametric form of the same problem and develop the improved MRAC scheme that works on normalized signal. Defining $W_b(s) = (sI - A_m)^{-1}B$, eq. (11) can be rewritten as

$$x(t) = W_b(s)\left[\theta^{*\mathrm{T}} x(t)\right] + W_b(s)[u(t)] \tag{14}$$

By the use of controllability properties and selecting a vector $c_0 \in \mathbb{R}^n$ so that $W_m(s) \triangleq c_0^T W_b(s)$ is a strictly proper minimum-phase transfer function, the parametric expression of the model is obtained as

$$z(t) = \theta^{*\mathrm{T}}\phi(t) \tag{15}$$

where $z(t) = c_0^T x(t) - W_m(s)[u(t)]$ and $\phi(t) = W_m(s)[x(t)]$ are available for measurements. The structure and parameters of the unmodeled dynamics are assumed unknown. As already mentioned, performance improvement is obtained by enriching the control signal with an auxiliary input u_a, which involves filtering of a feedback signal, as follows

$$u(t) = -\hat{\theta}^{\mathrm{T}}(t)x(t) + k_0 r(t) + u_a(t) \tag{16}$$

where
$$u_a(t) = -Q(s)\left[\epsilon m_s^2 + W_{c_0}(s)[\, W_b(s)[x^T(t)]\dot{\hat{\theta}}(t)]\right] \tag{17}$$

Herein $W_{c_0}(s) = -c_0^T(sI - A_m)^{-1},\ Q(s) = W_m(s)^{-1}/(\tau s + 1)^{n^*}$, and n^* is the relative degree of $W_m(s)$, while $\tau > 0$ is a design parameter. The associated adaptive algorithm is expressed as

$$\dot{\hat{\theta}}(t) = proj\big(P(\mathrm{t})\epsilon(t)\phi(t)\big), \qquad \hat{\theta}(0) = \hat{\theta}_0 \in \Omega \tag{18}$$

$$\dot{P}(t) = -P(t)\frac{\phi(t)\phi^T(t)}{m_s^2}P(t), \qquad P(0) = P_0 \tag{19}$$

where ϵ is the estimation error and is defined as $\epsilon(t) = \left(z(t) - \hat{\theta}^T\phi(t)\right)/m_s^2$. The normalizing signal is $m_s^2(t) = 1 + \phi^T(t)\phi(t)$, and it is designed to guarantee boundedness of $\left|\frac{\phi(t)}{m_s(t)}\right|$, independently whether $\phi(t)$ is bounded or not. Stability and convergence proof of this robust adaptive law are reported in [23]. For consistency, the reference model state matrix, the initial conditions, $\hat{\theta}$ convex set and $P(0)$ are set as the other control scheme. The design parameters are set as

$$\tau = 0.5; \qquad c_0 = \begin{bmatrix} 1 \\ 1 \end{bmatrix};$$

The design parameters are maintained unaltered with respect to the flap configuration for obvious consistency requirements in the adaptive law performance evaluation and validation. The only difference between the two control laws consist of an effectiveness parameter conversion acting on u. Spoilers accept as input a discrete value which range is 0 to 5, while trailing-edge flap input is a continuous value in degree bounded between $\pm$ 10 degree. For this reason a conversion look-up table, acting on the control signal, was introduced to convert the continuous value in the integer number of open spoilers that produce the corresponding aerodynamic effect.

IV. Simulation Results

The effectiveness of the architecture proposed is verified by an extensive set of simulations, of which the most relevant results are presented and discussed in this section. A trailing-edge flap configuration of the same wing section, coupled with the same modified MRAC adaptive controller is implemented and used as benchmark for a better evaluation of the obtained response. The geometrical, mass and inertial properties of the plant are reported in Table 1. The aerodynamics properties were already extensively discussed in Section II. Two significant sets of results are reported to show the efficacy of the architecture proposed.

A. Flutter and post-flutter closed loop response

The closed loop responses at flutter and post-flutter velocity are analyzed for both, multiple spoiler and trailing-edge flap control surface configurations and time histories of pitch angle and control signal are presented and compared. All the simulations are carried out inducing periodic LCOs by perturbing the dynamical system from its equilibrium condition by a pitch angle $\theta = 0.1\ rad$, at a fixed free stream velocity U equal or higher than the flutter threshold. In the first set of simulation, the effectiveness and robustness of the control action is evaluated by activating the controller at different time instant, which corresponds to different induced LCOs regimes. As was noted before, only the most meaningful results are reported hereafter, despite the large number of simulations performed. In particular, flutter $(U_{flutter} = 7.5\ m/s)$ and post-flutter $(U = 1.5 \cdot U_{flutter} = 11.25\ m/s)$ with controller activation at $t = 10\ sec$, which represent the most critical conditions of the first set of simulations, are analyzed and discussed. The numerical integration in all the simulations is performed using a fourth-order Runge-Kutta solver with a sampling time $t_s = 0.001\ sec$.

Figures 4 and Figure 5, clearly show that the proposed multiple spoilers' actuation strategy is able to effectively damp out flutter and post-flutter oscillations. In addition, the results obtained constitute a proof of robustness for the modified MRAC scheme designed with normalized signals. In fact, the results shows that the applied control law effectively converge with fast adaptation capabilities despite the high nonlinearities (structural and aerodynamic) and uncertainties (different control surface architecture) in the plant. Comparative analysis suggests that although convergence to zero is guaranteed, the spoiler configuration is more sensitive to wind speed increment. In the nominal

a, b	$-0.4, 0.135\ (m)$	$c_{l_\alpha}, c_{m_\alpha}$	$6.28, (0.5 + a)c_{l_\alpha}$
$k_\theta(\theta), k_h$	$\sum_{i=1}^{5} \tau_i \theta^{i-1}, 2844.4\ (N \cdot m^{-1})$	c_{l_β}, c_{m_β}	$3.358, -0.635$
ρ	$1.225\ (Kg \cdot m^3)$	$m_t = m_w$	$12.387\ kg$
τ_i	$[2.8\ \ -62.3\ \ 3709.7\ \ -24{,}195.6\ \ 48{,}756.9]^T$	I_θ	$0.065\ (kg \cdot m^2)$
c_θ, c_h	$0.036\ (N \cdot s), \qquad 27.43\ (N \cdot m^{-1} \cdot s^{-1})$	x_θ	$[0.0873 - (b + ab)]/b$

Table 1. 2D Aeroelastic Plant Parameters.

flutter condition, Figure 4, a time delay of about 3 second is observed. In the post-flutter simulation case reported in Figure 5, there is small performance deterioration shown by the spoiler solution. However, the absence of overshoot and steady state tracking error as well as a relatively fast transient, that is convergence obtained between 3 and 6 seconds from controller activation instant, are all proofs that a satisfactory response can be achieved in time domain by the proposed actuation solution. Moreover, since the spoilers are installed and operate only on one side of the wing, which means that are active only on one-half of the periodic oscillations, further considerations can be drawn as follows. Analyzing the control signals time history, where up to 5 spoilers have been used simultaneously, assuming an analogous power supply for both cases, the power consumption by the coordinated multiple spoiler actuation system is approximately 65% smaller than the standard flap configuration. This is a worthwhile saving when considering the application of the controller to an all-electric unmanned aircraft. Moreover, a combined action of the two actuations system could increase the efficacy and safety of damping the flutter avoiding saturation on the trailing edge flap control surface.

B. Closed loop response to gust

The second set of simulations concerns the robustness survey of the novel architecture to external disturbances that are different gust distributions. Similar to [17], three different velocity distributions of $w_g(\tau)$ are applied to the model, as reported in Figure 6. These are:

(a) Exponential graded gust

$$w_g(\tau) = H(\tau) w_0 \left(1 - e^{-\frac{0.75\tau}{3}}\right) \tag{20}$$

(b) Combined sinusoidal and random gust

$$w_g(\tau) = w_0 \sin(6\pi b\tau/U) + d_n H(\tau) \tag{21}$$

(c) Triangular gust of finite duration

$$w_g(\tau) = 2w_0 \frac{\tau}{\tau_G}\left(H(\tau) - H\left(\tau - \frac{\tau_G}{2}\right)\right) + 2w_0\left(\frac{\tau}{\tau_G} - 1\right)\left(H(\tau - \tau_G) - H\left(\tau - \frac{\tau_G}{2}\right)\right) \tag{22}$$

where $H(\cdot)$ is the Heaviside function, commonly defined as

$$H(x) = 0 \quad if\ x < 0; \qquad \frac{1}{2} \quad if\ x = 0; \qquad 1 \quad if\ x > 0 \tag{23}$$

and $\tau_G = Ut_G/b, \quad t_G = 0.5\ sec$ is the dimensionless time of the gust. $w_0 = 0.07$ for case (a) and (b), while in case (c) $w_0 = 0.7$. The random component in case (b) $d_n H(\tau)$ is obtained by passing white noise with unit variance through a filter defined by its transfer function as $F_d(s) = 10^{-5}/(s + 5)$. For all the three case reported, the plant simulation parameters are set to represent the worst case scenario for the model under examination: the free stream velocity is $U = 1.5\ U_{flutter} = 11.25\ m/s$, $\theta(0) = 0.1\ rad$ and the controller is on at time zero, in the presence of the gust action. Figures 7 and 8, respectively, show the pitch angle and control signal time histories demonstrate the robustness of the control architecture proposed. The spoilers are able to counteract all of the external gust disturbances with extremely small changes in the response, both for pitch angle and control action. The considerable increment of pitching moment, generated by the coordinated multiple spoiler strategy, makes the transient response almost unaffected by the different gusts applied. However, small residual oscillations about the equilibrium position or small drift from the zero angles can be observed in the time-history graphs. This is due to the spoiler binary action of the model, which create a dead zone of activation for a pitch angle less than 0.5 degrees.

Nevertheless, this is a negligible vibration behavior for the wing and the issue can be easily solved by implementing a gradual opening strategy at least for the first spoiler.

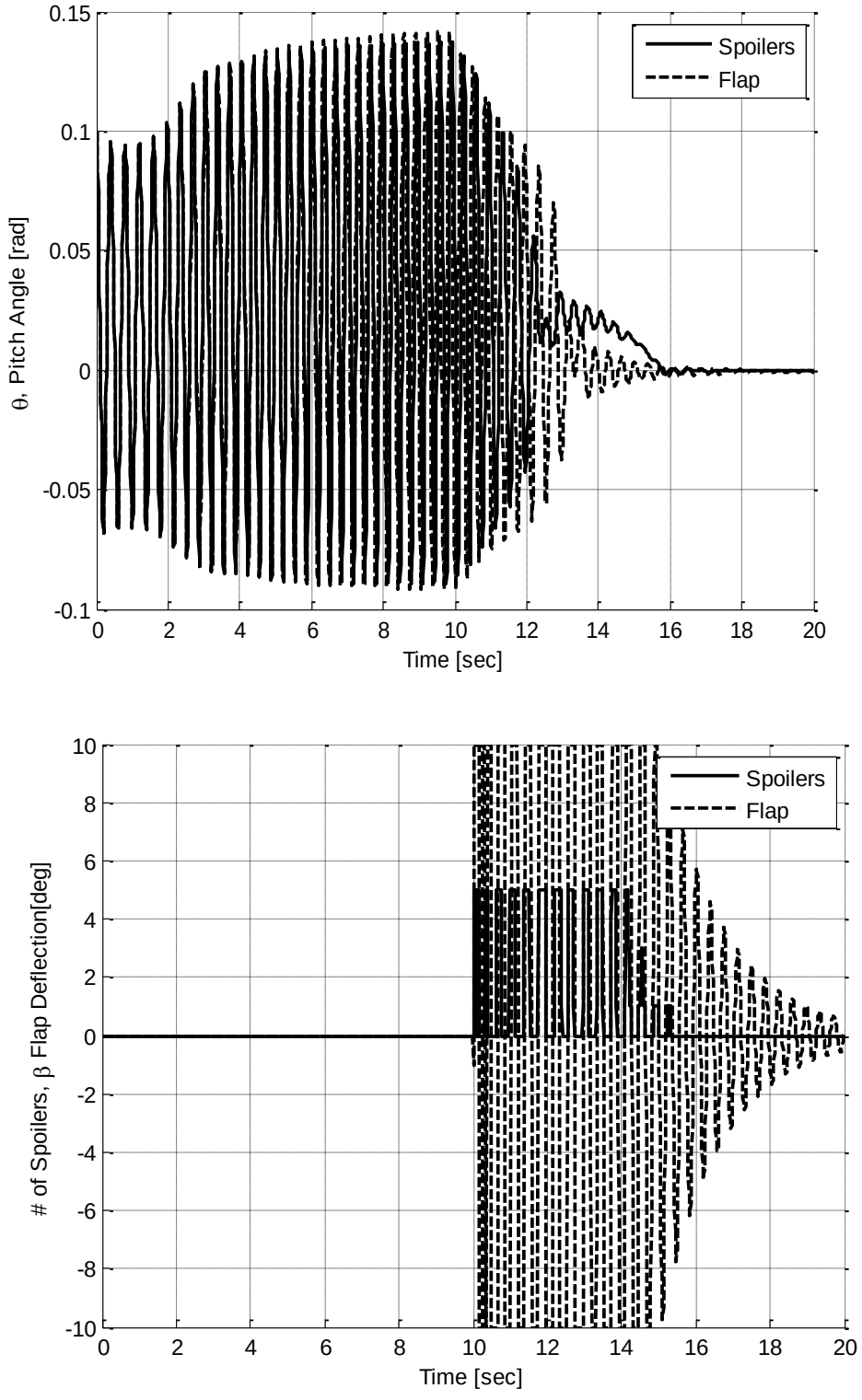

Figure 4. Pitch Angle and Actuation Time Histories Comparison. *Flutter condition***.**

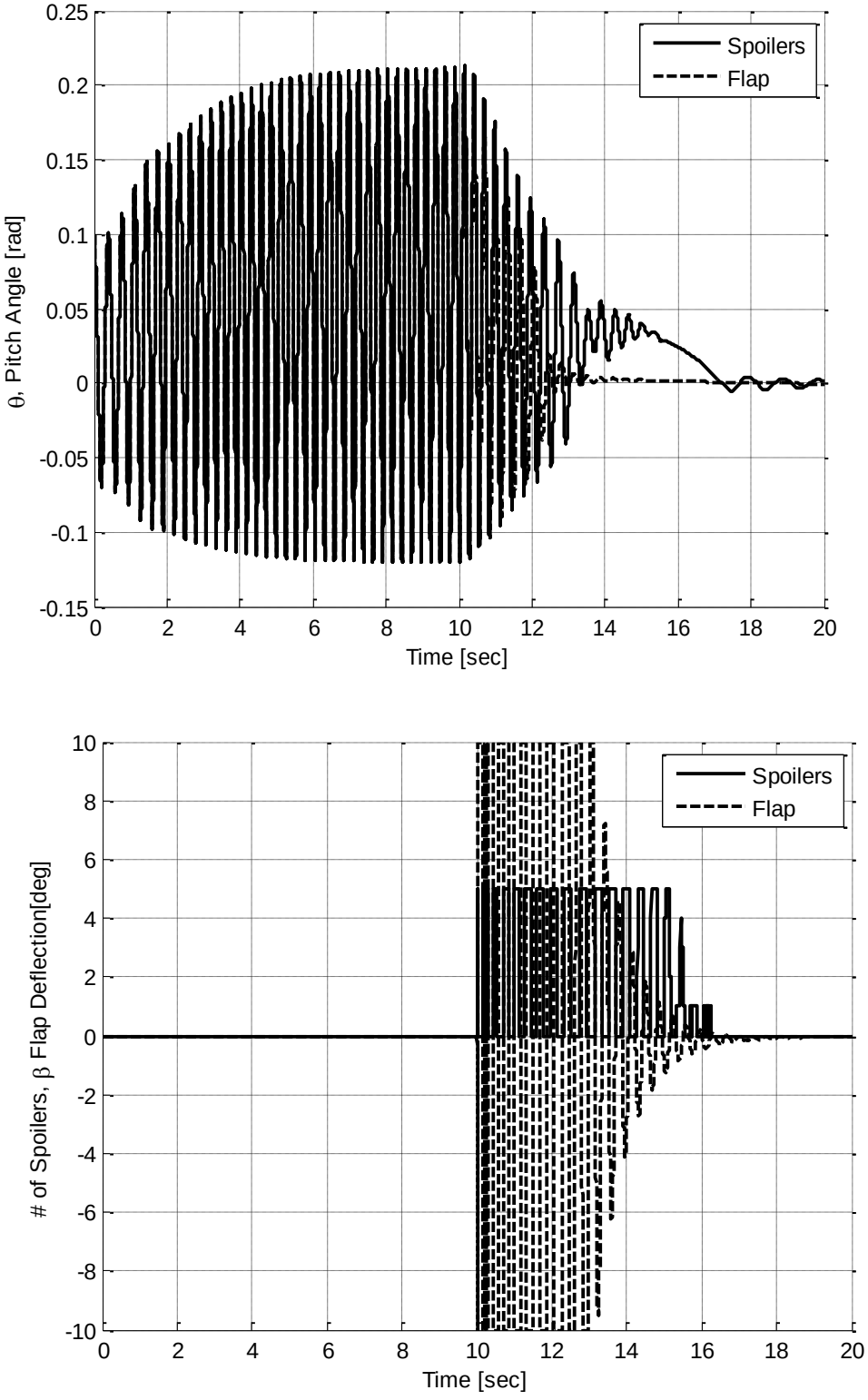

Figure 5. Pitch Angle and Actuation Time Histories Comparison. *Post-Flutter condition*.

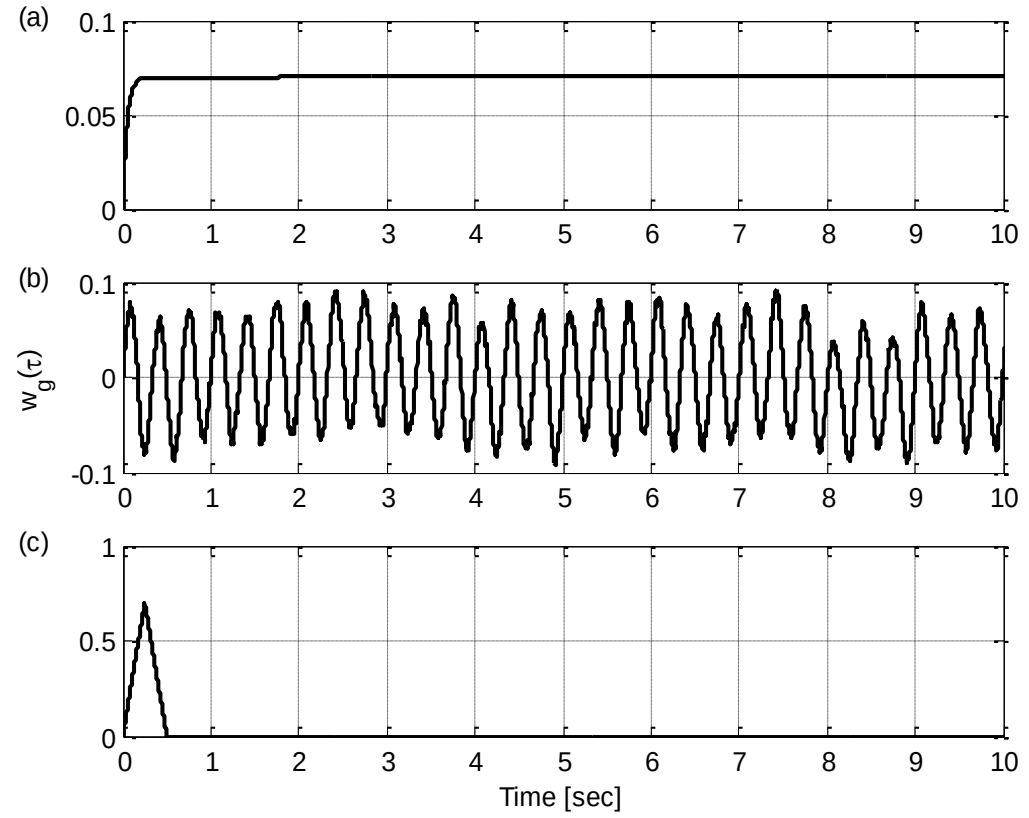

Figure 6. External disturbance velocity w_g (τ). *(a) exponential graded gust, (b) combined sinusoidal and random gust, (c) triangular gust***.**

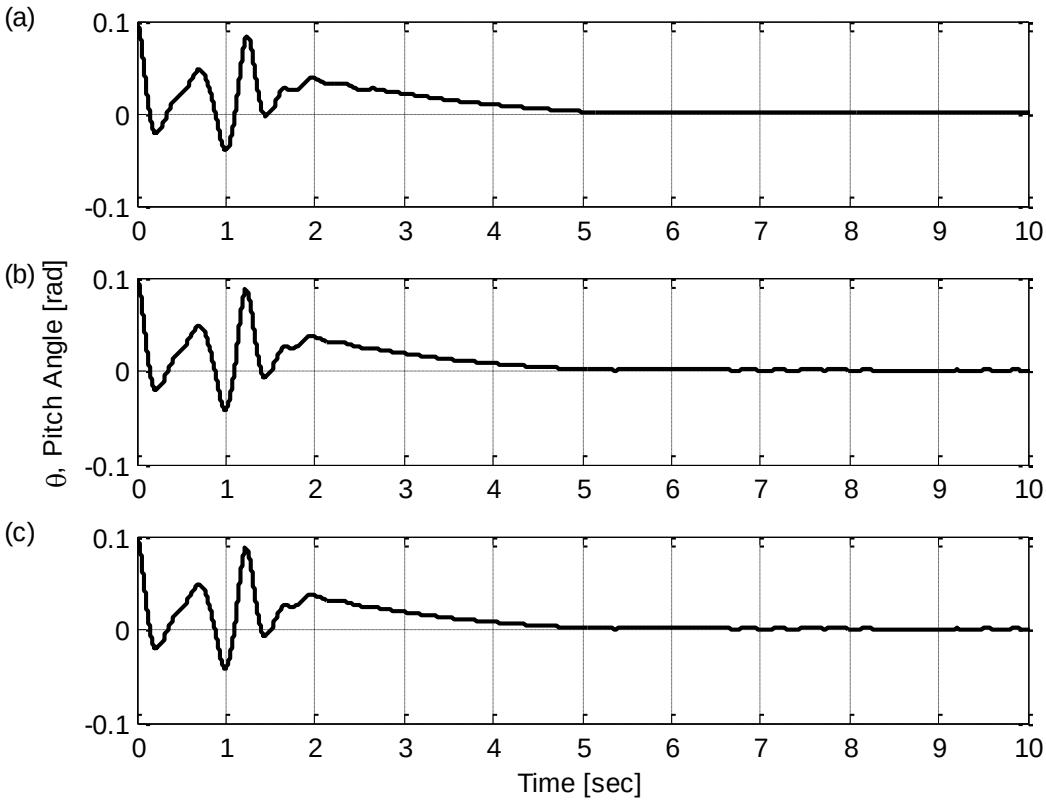

Figure 7. Pitch angle time history of the closed loop response. *(a) exponential graded gust, (b) combined sinusoidal and random gust, (c) triangular gust.*

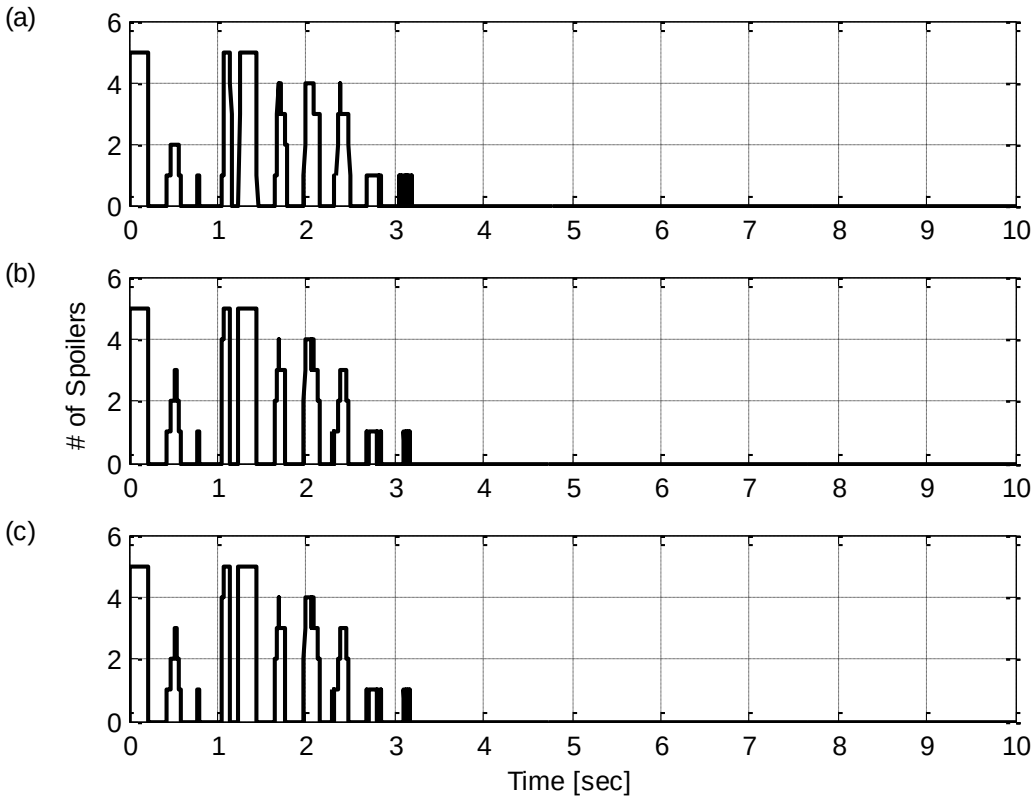

Figure 8. Spoiler actuation time histories for the cloosed loop response. *(a) exponential gust, (b) combined sinusoidal and random gust, (c) triangular gust*.

V. Conclusions

In this paper, a multiple spoiler configuration, with predefined and coordinated actuation strategy, designed to control flutter and post-flutter limit cycle oscillations is presented. Based on computational fluid dynamics (CFD) studies, the proposed wing-spoiler configuration is fabricated and tested in the wind tunnel to obtain the nonlinear aerodynamic database implemented in the simulation model. A well-known, preexisting plunging/pitching nonlinear structural model is adopted for the aeroelastic system. The same aeroelastic plant is modified to account for trailing-edge control surface effect, which is used for validation and results comparison purpose. A normalized model reference adaptive control (MRAC) scheme, modified for performance improvement, is applied to both plants and regulation of the states dynamics to zero is obtained with the same control algorithm, which provides additional validation proofs to the scheme's robustness and adaptation capabilities. Comparison of performances demonstrates that the spoiler control architecture represent a viable alternative and can even surpass the standard trailing-edge flap controller by providing energy saving and additional safety. In addition, sensitivity analysis to external gust disturbances is performed with positive outcomes that confirm the effectiveness of the control architecture proposed. Further analyses, as a multi-input multi-output control of the same aeroelastic system with combined action of spoilers and flap, are planned as future work.

Acknowledgments

The authors would like to thank the EU Research Executive Agency (REA) for supporting the A2 Net Team project under FP7 Marie Curie Grant 269190. The A2 Net Team project established a connection among the authors of the paper and created an environment in which the authors have done much of the work presented here. Partial support for this research and facilities where most of the wind tunnel testing presented in this paper was conducted were provided by the School of Engineering of Clarkson University.

References

[1] Dowell, E.H., *A Modern Course in Aeroelasticity*, Sijthoff and Noordhoff, 1978, Ch. 5.
[2] Fung, Y.C., *An Introduction to the Theory of Aeroelasticity*, Dover, New York, 1955, Ch. 3, 5, 9, 13-15.

[3] Bisplinghoff, R.L., Ashley, H., Halfman, R.L., *Aeroelasticity*, Dover, New York, 1996, Ch. 6-10.
[4] Waszak, M.R., "Robust Multivariable Flutter Suppression for Benchmark Active Control Technology Wind-Tunnel Model", *Journal of Guidance, Control, and Dynamics*, Vol. 24, No. 1, 2001, pp. 147-153. doi: 10.2514/2.4694
[5] Mukhopadhyay, V., "Transonic Flutter Suppression Control Law Design and Wind-Tunnel Test Results", *Journal of Guidance, Control and Dynamics*, Vol. 23, No. 5, 2000, pp. 930-937. doi: 10.2514/2.4635
[6] Kelkar, A.G., and Joshi, S.M., "Passivity-Based Robust Control with Application to Benchmark Controls Technology Wing", *Journal of Guidance, Control and Dynamics*, Vol. 23, No. 5, 2000, pp. 938-947. doi: 10.2514/2.4636
[7] Block, J.J., and Strganac, T.W., "Applied Active Control for a Nonlinear Aeroelastic Structure", *Journal of Guidance, Control, and Dynamics*, Vol. 21, No. 6, 1998, pp. 838-845. doi: 10.2514/2.4346
[8] Platanitis, G., and Strganac, T.W., "Control of a Nonlinear Wing Section Using Leading- and Trailing-Edge Surfaces", *Journal of Guidance, Control, and Dynamics*, Vol. 27, No. 1, 2004, pp. 52-58. doi: 10.2514/1.9284
[9] Platanitis, G., and Strganac, T.W., "Suppression of Control Reversal Using Leading- and Trailing-Edge Control Surfaces", *Journal of Guidance, Control, and Dynamics*, Vol. 28, No. 3, 2005, pp. 452-460. doi: 10.2514/1.6692
[10] O'Neil, T., and Strganac, T.W., "Aeroelastic Response of a Rigid Wing Supported by Nonlinear Springs", *Journal of Aircraft*, Vol. 35, No. 4, July–August 1998, pp. 616-622. doi: 10.2514/2.2345
[11] Cassaro, M., Battipede, M., Marzocca, P., Behal, A., "A Comparison of Adaptive Control Architectures for Flutter Suppression*", Journal of Guidance, Control, and Dynamics,* doi: 10.2514/1.G000707.
[12] Gujjula, S., Singh, S.N., Yim, W., "Adaptive and Neural Control of a Wing Section Using Leading- and Trailing-Edge Surfaces", *Aerospace Science and Technology*, Vol. 9, No. 2, 2005, pp. 161-171.
[13] Behal, A., Marzocca, P., Rao, V.M., Gnann, A., "Nonlinear Adaptive Control of an Aeroelastic Two-Dimensional Lifting Surface", *Journal of Guidance, Control, and Dynamics*, Vol. 29, No. 2, March-April 2006, pp. 382-390. doi: 10.2514/1.14011
[14] Cassaro, M., Battipede, M., Cestino, E., Marzocca, P., Behal, A., "$\mathcal{L}_1$ adaptive flutter suppression control strategy for highly flexible structure", *SAE Int. J. Aerosp*., Vol. 6, No. 2, December 2013. doi:10.4271/2013-01-2263
[15] Cassaro, M., Nágy, A., Marzocca, P., Battipede, M., Ahmadi, G., "Novel Active Control Strategy for LCO and Flutter Suppression by a Coordinated Use of Multiple Distributed Surface Actuators", *Proceedings of the ASME 2014 International Mechanical Engineering Congress & Exposition*, IMEC2014, November 14-20, 2014, Montreal, Quebec, Canada.
[16] Wagner, H., "Uber die Entstehung des dynamischen Auftriebes von Tragflugeln", *Zeitschrift fur Angewandte Mathematic und Mechanik*, 5(1):17–35, 1925.
[17] Theodorsen, T., "General Theory of Aerodynamic Instability and the Mechanism of Flutter," NACA Rept. 496, 1935.
[18] Sheta, E.F., Harrand, V.J., Thompson, D.E., Strganac T.W., "Computational and Experimental Investigation of Limit Cycle Oscillations of Nonlinear Aeroelastic Systems", *Journal of Aircraft*, Vol. 39, No. 1, January–February 2002. doi: 10.2514/2.2907
[19] Behal, A., Marzocca, P., Rao, V.M., Gnann, A.," Nonlinear Adaptive Control of an Aeroelastic Two-Dimensional Lifting Surface", *Journal of Guidance, Control, and Dynamics*, Vol. 29, No. 2, March-April 2006, pp. 382-390. doi: 10.2514/1.14011
[20] Ko, J., Strganac, T.W., Kurdila, A.J., "Stability and Control of a Structurally Nonlinear Aeroelastic System", *Journal of Guidance, Control, and Dynamics*, Vol. 21, No. 5, 1998, pp. 718–725. doi: 10.2514/2.4317
[21] Singh, S.N., Wang, L., "Output Feedback Form and Adaptive Stabilization of a Nonlinear Aeroelastic System," *Journal of Guidance, Control, and Dynamics*, Vol. 25, No. 4, 2002, pp. 725–732. doi: 10.2514/2.4939
[22] Hanke, C.R., Nordwall, D.R., *The Simulation of a Jumbo Jet Transport Aircraft*, D6-30643, Volume II: Modeling Data, The Boeing Company, Wichita Division, September 1970, Wichita, Kansas.
[23] Ioannou, P.A. and Sun, J., *Robust Adaptive Control*, upper Saddle River, NY: Prentice Hall, 1989, Ch. 9.
[24] Wang, Z., Behal, A., and Marzocca, P., "Model-Free Control Design for Multi- Input Multi-Output Aeroelastic System Subject to External Disturbance," *Journal of Guidance, Control, and Dynamics*, Vol. 34, No. 2, 2011, pp. 446-458. doi: 10.2514/1.51403.